

# AGN must be very efficient at powering outflows

Kastytis Zubovas<sup>1,2,\*</sup>

<sup>1</sup>Center for Physical Sciences and Technology, Saulėtekio av. 3, Vilnius LT-10257, Lithuania

<sup>2</sup>Astronomical Observatory, Vilnius University, Saulėtekio av. 3, Vilnius LT-10257, Lithuania

\* E-mail: kastytis.zubovas@ftmc.lt

11 September 2021

## ABSTRACT

Galaxy evolution is affected by competing feedback processes. Stellar feedback dominates in low-mass galaxies, while AGN feedback predominantly affects massive ones. Recent observational results reveal the dependence of black hole accretion rate (BHAR) and star formation rate (SFR) on galaxy stellar mass, and give information on the galaxy mass at which the changeover between dominant feedback mechanisms occurs. I use this information to derive an empirical estimate of the coupling efficiency,  $f_{\text{AGN}}$ , between AGN luminous energy output and AGN-driven galactic outflows, and the momentum loading factor  $f_{\text{p,AGN}}$  between the momentum of AGN radiation field and the outflow. The results are independent of any particular model of AGN feedback and show that AGN feedback must be very efficient and/or have very large momentum loading in order to explain current observations. I discuss possible ways of reaching the required efficiency and loading factor, and the selection effects that might result in only weak outflows being observed, while the most powerful ones may be generally obscured. There are significant uncertainties involved in the derivation of the result; I suggest ways of reducing them. In the near future, better estimates of coupling efficiency can help distinguish among AGN feedback models, investigate the redshift evolution and mass dependence of feedback efficiency.

**Key words:** galaxies: active — accretion, accretion discs — galaxies: evolution — ISM: evolution — supernovae: general — stars: winds, outflows

## 1 INTRODUCTION

Stellar and active galactic nuclei (AGN) feedback is a crucial component of galaxy evolution (Shankar et al. 2006; Kormendy & Ho 2013; Somerville & Davé 2015). Cosmological simulations show that the present-day galaxy mass function and its redshift evolution can only be explained when the effects of feedback are included (Vogelsberger et al. 2014; Schaye et al. 2015). The two sources of feedback are important over different mass ranges; in particular, stellar feedback regulates the processes in low-mass galaxies while large galaxies are mainly regulated by AGN feedback (Shankar et al. 2006; Kormendy et al. 2009; Schaye et al. 2010; Heckman & Best 2014).

The galaxy stellar mass at which the two processes become comparably important can inform our understanding of the efficiency with which feedback processes operate. This mass has been usually associated with the ‘break’ seen in the galaxy mass function ( $M_{\text{br}} \sim 1.2 \times 10^{10} M_{\odot}$ ; Shankar et al. 2006) or, equivalently, the maximum of the stellar-to-halo mass ratio ( $M_{\text{br}} \sim 2 \times 10^{10} M_{\odot}$ ; Behroozi et al. 2013). Recently, a similar break was discovered in the  $M_{\text{BH}} - \sigma$

relation between supermassive black hole (SMBH) mass and host galaxy spheroid velocity dispersion, which corresponds to a transition mass  $M_{\text{tr}} = 3.4 \pm 2.1 \times 10^{10} M_{\odot}$  (Martin-Navarro & Mezcua 2018).

A straightforward interpretation of this break, or transition, mass is that in galaxies with lower stellar mass, stellar feedback injects more energy than AGN feedback into the interstellar medium (ISM) over the lifetime of the galaxy, while in more massive galaxies, the opposite is true. In more massive galaxies, therefore, galaxy properties are more tightly correlated with properties of the SMBH, while in less massive galaxies, this correlation is weaker and SMBH mass depends less strongly on galaxy mass. Both stellar and AGN feedback power are proportional to the corresponding mass flow rate  $\dot{M}$ : the star formation rate (SFR) for stellar feedback and the black hole accretion rate (BHAR) for AGN. Recent discoveries that the average BHAR-to-SFR ratio increases with increasing galaxy stellar mass (Yang et al. 2017, 2018) suggests a simple explanation that even if stellar and AGN feedback processes act identically in galaxies across the mass range, AGN feedback can become dominant for galaxies with large stellar mass.

This interpretation offers a possibility to constrain the efficiencies of stellar or AGN feedback coupling, i.e. the fractions of stellar or AGN luminous energy output that is transferred to the ISM of the host galaxy. Stellar feedback has been investigated in significant detail (e.g., Leitherer et al. 1992; Thornton et al. 1998; Murray et al. 2005; Walch & Naab 2015), leading to a good understanding of the energetics of the process. AGN feedback, on the other hand, is less well understood, with models producing different predictions of coupling efficiency (e.g., King 2003; Sazonov et al. 2005; Murray et al. 2005; Zubovas & King 2012; Ishibashi et al. 2018) and observations calling various theoretical scenarios into question.

In this paper, I derive a model-independent constraint on the coupling efficiency between the AGN luminous energy output and the gas in the host galaxy,  $f_{\text{AGN}}$ , averaged over the Hubble time. This efficiency turns out to be very high,  $f_{\text{AGN}} > 0.045$ . This implies that most galaxy quenching via AGN outflows happened at high redshift and that most massive galactic outflows seen today are far less efficient than they should have been in high redshift galaxies, or that stellar feedback is much less efficient than generally assumed. I suggest ways of testing these findings and discuss their importance in distinguishing among AGN feedback models.

## 2 AGN FEEDBACK COUPLING EFFICIENCY

In order to compare the effects of stellar feedback and AGN feedback, I consider the injection of energy and/or momentum by these processes into the ISM integrated over the lifetime of the galaxy. This approach is also advantageous, because it doesn't require any detailed analysis of the star formation or accretion histories of the galaxy, but merely the time-integrated or averaged values of  $\dot{M}$ . Furthermore, injection of energy which is efficiently radiated away can be neglected by considering the long-term coupling efficiencies of feedback energy to the ISM, and momentum injection can be treated in a similar fashion.

Here, I first consider the injection of energy and derive the AGN energy coupling efficiency which is required in order to explain the observed break in the galaxy mass function (Section 2.1). Next, I use an analogous argument to derive the required momentum loading factor (Section 2.2) and present the expected variation of these factors with redshift (Section 2.3).

### 2.1 Energy coupling

Energy injection into the ISM comes primarily from two sources: stars and active nuclei. The total amount of injected AGN energy,  $E_{\text{AGN}}$ , integrated over the lifetime of the galaxy, depends on three factors: the BHAR  $\dot{M}_{\text{BH}}$ , the radiative efficiency  $\epsilon_{\text{AGN}}$  of converting the mass into energy, and the coupling efficiency  $f_{\text{AGN}}$  between the radiative energy output and the ISM:

$$E_{\text{AGN}} = \int_0^{t_{\text{H}}} f_{\text{AGN}} \epsilon_{\text{AGN}} \dot{M}_{\text{BH}} c^2 dt, \quad (1)$$

where  $t_{\text{H}}$  is the Hubble time. Stellar feedback comprises feedback at different stages in the star's life, but is also, on long

timescales, proportional to the total stellar mass formed:

$$E_* = \sum_i \int_0^{t_{\text{H}}} f_{*,i} \epsilon_{*,i} \dot{M}_* dt, \quad (2)$$

where the index of summation goes over the different feedback processes,  $\dot{M}_*$  is the star formation rate and  $\epsilon_{*,i}$  is the energy release per unit mass formed for the different processes. The product  $\epsilon_{*,i} \dot{M}_*$  then gives the energy injection rate by stellar feedback of a particular type. The ratio of energy input by AGN feedback to that of stellar feedback is then

$$R \equiv \frac{f_{\text{AGN}} L_{\text{AGN}}}{\sum_i P_{*,i}} = \frac{f_{\text{AGN}} \epsilon_{\text{AGN}} c^2 \dot{M}_{\text{BH}}}{\sum_i f_{*,i} \epsilon_{*,i} \dot{M}_*}, \quad (3)$$

where the integration used in equations (1) and (2) can be removed since the limits are identical. I also used  $L_{\text{AGN}} = \epsilon_{\text{AGN}} \dot{M}_{\text{BH}} c^2$  and  $P_{*,i} = f_{*,i} \epsilon_{*,i} \dot{M}_*$  for conciseness. I will now derive the numerical value of  $f_{\text{AGN}}$  from the preceding equation, based on the following assumptions:

- Galaxies with  $R < 1$  are dominated by stellar feedback, while galaxies with  $R > 1$  are dominated by AGN feedback; therefore, there is a transition at  $R = 1$ , which is observable as the break in the galaxy luminosity function, the peak of the stellar-to-halo mass ratio, and the break in the black hole mass - velocity dispersion relation. A difference of the dominating feedback process is the conventional explanation of the shape of the galaxy stellar mass function (see, e.g., Puchwein & Springel 2013; Moster et al. 2013; Harrison 2017).

- The radiative and feedback coupling efficiencies of AGN do not depend systematically on galaxy stellar mass. They might depend, directly or indirectly, on the gas content of the galaxy, but I argue below that the galaxy mass function must have been established at high redshift, when gas content was large in all galaxies.

- The feedback energy per unit mass of stars formed, and the coupling of this energy to the ISM, do not depend systematically on galaxy mass. This is not necessarily completely true, but I show below that the possible dependence is smaller than the dependence of BHAR and SFR on galaxy mass.

- Only the fraction of input energy which is efficiently coupled to the large-scale ISM is considered. This means that energy that is efficiently radiated away, as well as energy that is fully dissipated on small scales, is not taken into account.

With these assumptions,  $R$  depends on galaxy mass only through the BHAR-to-SFR ratio, while the other factors in eq. (3) are all constant. There are various estimates for these constant factors in the literature, which I outline below.

There are essentially two important modes of stellar feedback: winds and supernovae (radiation pressure is unlikely to be very important; see, e.g., Rosdahl et al. 2015). Stellar wind feedback power, assuming a continuous star formation episode, is

$$P_w \simeq 3 \times 10^{41} f_{w,p} \frac{\dot{M}_*}{M_{\odot} \text{yr}^{-1}} \text{ergs}^{-1}, \quad (4)$$

where  $0.3 < f_{w,p} < 1$  is an efficiency factor encompassing the various uncertainties of wind production models

(Leitherer et al. 1992). The wind coupling efficiency  $f_{w,c}$  is less constrained, especially on scales larger than the star-forming regions. Observational estimates suggest mechanical energy coupling on star-forming region scale of  $0.037 < f_{w,c} < 0.38$  (Rosen et al. 2014), while numerical simulations suggest a combined kinetic and thermal energy retention of  $0.23 < f_{w,c} < 0.48$  at the end of a star's wind phase (Fierlinger et al. 2016). The combined factor  $f_w \equiv f_{w,p} f_{w,c}$  can then have values  $0.011 < f_w < 0.48$ , however the lower end of this range appears unlikely due to being estimated on smaller scales than the whole galaxy. I will therefore adopt a range  $0.2 < f_w < 0.5$ .

Supernova feedback can be estimated from either an energy argument or a momentum argument. The energy estimate gives

$$P_{SN} \simeq 3 \times 10^{41} f_{SN} \frac{\dot{M}_*}{M_{\odot} \text{yr}^{-1}} \text{ergs}^{-1}, \quad (5)$$

where  $f_{SN} < 1$  is the very uncertain coupling efficiency, and a Chabrier (2003) mass function is used, giving a supernova rate  $\dot{N}_{SN} = 0.01$  per Solar mass formed. A more robust estimate can be attained by using the calculation in Murray et al. (2005), assuming momentum injection and taking the terminal velocity of the wind to be approximately the velocity dispersion in the galaxy:

$$P_{SN} \simeq \dot{p}_{SN} \sigma_{gal} \simeq 3 \times 10^{40} \frac{\dot{M}_*}{M_{\odot} \text{yr}^{-1}} v_{200} \text{ergs}^{-1}, \quad (6)$$

where  $v_{200}$  is the rotational velocity of the galaxy  $v_{rot}$  in units of  $200 \text{ km s}^{-1}$  and I assume  $\sigma_{gal} = v_{rot}/\sqrt{2}$ . Combining this expression with eq. (5), I get  $f_{SN} \simeq 0.1 v_{200}$ . Numerical simulations of individual and paired supernova explosions in various ISM geometries give values  $0.05 < f_{SN} < 0.4$  (Thornton et al. 1998; Walch & Naab 2015). The highest efficiencies are reached on short timescales or in simulations with multiple supernovae or in pre-ionised clouds, so the average value should be smaller. In the following, I will use a range  $0.05 < f_{SN} < 0.2$ . This range agrees well with the analytical estimate above, at least for galaxies with  $0.5 < v_{200} < 2$ . Using the baryonic Tully-Fisher relation (Tully & Fisher 1977), this range of velocities corresponds to galaxy stellar masses  $5 \times 10^9 M_{\odot} < M_* < 1.3 \times 10^{12} M_{\odot}$  (McGaugh 2005), easily encompassing the allowed range of SMBH scaling transition mass (Martin-Navarro & Mezcua 2018) and the break in the galaxy mass function (Behroozi et al. 2013). Therefore the possible scaling of  $f_{SN}$  with galaxy mass via the terminal velocity of SN-driven winds is unlikely to play a major role in determining the transition mass between stellar- and AGN-feedback dominated galaxies.

The radiative power of luminous AGN is

$$L_{AGN} = \epsilon_{AGN} \dot{M}_{BH} c^2 = 5.7 \times 10^{45} \epsilon_{0.1} \frac{\dot{M}_{BH}}{M_{\odot} \text{yr}^{-1}} \text{ergs}^{-1}, \quad (7)$$

where I parameterize  $\epsilon \equiv 0.1 \epsilon_{0.1}$ . The feedback power injected into the ISM is then  $f_{AGN} L_{AGN}$ .

Putting these expressions into eq. 3 gives

$$R \simeq 1.9 \times 10^4 \frac{f_{AGN} \epsilon_{0.1}}{f_w + f_{SN}} \frac{\dot{M}_{BH}}{M_*}. \quad (8)$$

This equation can be rearranged to give  $f_{AGN}$ :

$$f_{AGN} \simeq 5.3 \times 10^{-5} R \frac{f_w + f_{SN}}{\epsilon_{0.1}} \frac{\dot{M}_*}{\dot{M}_{BH}}. \quad (9)$$

By definition,  $R = 1$  for galaxies where stellar and AGN feedback is equally important. Using the transition mass  $M_{tr} \sim 3.4 \times 10^{10} M_{\odot}$  (Martin-Navarro & Mezcua 2018) gives a BHAR/SFR ratio  $10^{-4} < \dot{M}_{BH}/\dot{M}_* < 3 \times 10^{-4}$ , increasing with redshift (Yang et al. 2017, 2018). Expressing this as a scaled relation  $\dot{M}_{BH}/\dot{M}_* = 3 \times 10^{-4} f_a$ , with the scaling parameter  $0.3 < f_a < 1$ , leads to

$$f_{AGN} \simeq 0.18 \frac{f_w + f_{SN}}{\epsilon_{0.1} f_a}. \quad (10)$$

The full range of the adopted values of  $f_w$ ,  $f_{SN}$  and  $f_a$  leads to a range for  $f_{AGN}$ :

$$0.045 < f_{AGN} < 0.42. \quad (11)$$

## 2.2 Momentum-loading factor

The above estimate has several inherent uncertainties, all related to the coupling between injected energy and the ISM. An uncertain amount of energy can be radiated away, and this fraction depends on the details of the ISM. The interaction of stellar and AGN feedback can also have unpredictable effect. It is impossible to eliminate these uncertainties without detailed numerical simulations. On the other hand, a similar estimate can be made by considering momentum injection by both stars and AGN.

Stars mainly inject momentum via winds and supernova explosions. Direct radiation pressure has a powerful, but mainly local, effect in disrupting dense molecular clouds, but later rapidly leaks out and does not couple very strongly to the galactic-scale ISM (Agertz et al. 2013). Wind momentum injection is  $p_w \simeq 2.34 \times 10^{40} \text{ g cm s}^{-1}$  per Solar mass (Agertz et al. 2013), which translates to

$$\dot{p}_w = 7.43 \times 10^{32} f_{p,w} \frac{\dot{M}_*}{M_{\odot} \text{yr}^{-1}} \text{g cm s}^{-2}, \quad (12)$$

where  $f_{p,w} \simeq 1$  is the wind momentum loading factor. The momentum injection rate from supernovae is

$$\dot{p}_{SN} = 6.3 \times 10^{32} f_{p,SN} \frac{\dot{M}_*}{M_{\odot} \text{yr}^{-1}} \text{g cm s}^{-2}, \quad (13)$$

where  $f_{p,SN} \simeq 8 - 25$  is the supernova momentum-loading factor (Agertz et al. 2013; Martizzi et al. 2015; Walch & Naab 2015).

Using these values for stellar momentum injection, AGN momentum injection  $\dot{p}_{AGN} = f_{p,AGN} L_{AGN}/c$  and the fact that at transition mass, the two should be equal, leads to an estimate for  $f_{p,AGN}$ :

$$f_{p,AGN} \simeq 3.3 \times 10^{-3} \frac{1.18 f_{p,w} + f_{p,SN}}{\epsilon_{0.1}} \frac{\dot{M}_*}{\dot{M}_{BH}}, \quad (14)$$

where the factor  $1.18 \simeq 7.43/6.3$  is used to scale the wind momentum injection rate to that of supernovae. Using the values of  $f_{p,w}$ ,  $f_{p,SN}$  and the BHAR/SFR ratio leads to a range of  $f_{p,AGN}$ :

$$100 < f_{p,AGN} < 830. \quad (15)$$

## 2.3 Redshift dependence

Both expressions for AGN coupling have redshift dependence which arises from the variation of the BHAR/SFR ratio with redshift. At high redshift, the ratio is typically

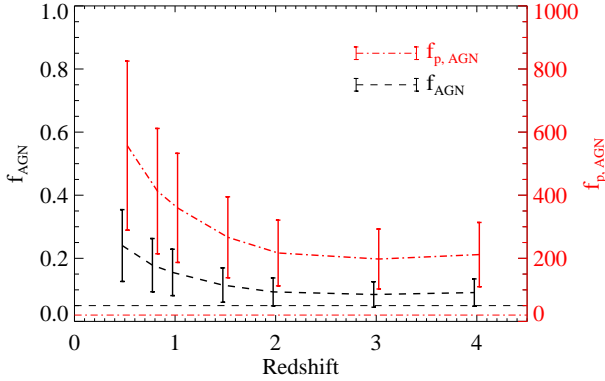


**Figure 1.** Required AGN energy coupling efficiency (black dashed line, left scale) and AGN momentum loading factor (red dash-dotted line, right scale) as function of redshift. Error bars represent the estimated range at each redshift, lines connect the mean values at each redshift. For clarity, the bars are offset horizontally by  $\Delta z = \pm 0.025$ . Horizontal lines represent analytical estimates of energy-driven AGN outflows:  $f_{\text{AGN}} = 0.05$  and  $f_{\text{p,AGN}} = 20$ .

larger, therefore the AGN coupling efficiency or momentum loading factor can be smaller and still produce the correct transition mass. Using the minimum and maximum BHAR/SFR ratios at  $M_* = M_{\text{tr}}$  leads to the following results:

- At  $z \simeq 0.5$ ,  $0.13 < f_{\text{AGN}} < 0.42$  and  $290 < f_{\text{p,AGN}} < 830$ ;
- At  $z \simeq 3$ ,  $0.045 < f_{\text{AGN}} < 0.13$  and  $100 < f_{\text{p,AGN}} < 290$ ;

Estimates of  $f_{\text{AGN}}$  and  $f_{\text{p,AGN}}$  for all redshift bins considered in Yang et al. (2018) are shown in Figure 1.

### 3 DISCUSSION

The foremost implication of the derived range of  $f_{\text{AGN}}$  values is that the coupling between AGN luminosity and the ISM should, on average, be very large. Although I find  $f_{\text{AGN}} < 1$ , which means the estimate is possible on energy conservation grounds, the value is generally larger than typical theoretical predictions and significantly larger than observational estimates. Theoretical models of AGN wind-driven outflow feedback (King 2010; Zubovas & King 2012) and radiation pressure feedback (Ishibashi et al. 2018) predict  $f_{\text{AGN}} \sim 5\%$  under idealised conditions, the same value is used in cosmological numerical simulations (Booth & Schaye 2009; Schaye et al. 2015). Numerical simulations of more realistic clumpy medium (Bourne & Zubovas 2018, submitted), as well as observations of real outflows (Fiore et al. 2017) suggest even lower values  $f_{\text{AGN}} < 1\%$ .

The required momentum loading factor shows much greater tension with analytical predictions and observations. Models typically predict  $f_{\text{p,AGN}} \sim 20$ , a factor 5 lower than the lowest value estimated here, although the scatter in analytical predictions is larger than for  $f_{\text{AGN}}$  (Zubovas & King 2012).

There are several potential ways to reconcile this tension. I first consider the explanations based on assuming the estimated values of  $f_{\text{AGN}}$  and  $f_{\text{p,AGN}}$  are approximately correct and later discuss the possibility that they are significant and systematic over-estimates of real values.

#### 3.1 Possibility of reaching high $f_{\text{AGN}}$ and $f_{\text{p,AGN}}$

The derived coupling efficiency requires that a significant fraction, much higher than 1%, of AGN luminous energy output is efficiently coupled to the host galaxy ISM. The momentum loading factor similarly suggests that the outflow should propagate in an ISM with very high optical depth, which would lead to photons scattering many times before escaping the galaxy, increasing the scalar momentum of the outflowing gas. There are two ways of achieving this result.

One possibility is hyper-Eddington SMBH growth during Compton-thick (heavily obscured) phases. In this case, most of the radiated energy can couple to the ISM, producing warm absorbers (King & Pounds 2014; King & Muldrew 2016). This energy can couple to the ISM surrounding the AGN in multiple ways - via winds, radiation pressure, gas heating or jets. The precise mechanism of this coupling is not important for the purpose of this discussion, so long as it results in  $f_{\text{AGN}} \sim 1$  during that stage of SMBH growth. If heavily obscured accretion results in the SMBH growing by  $\Delta M_{\text{obs}}$  throughout the lifetime of the galaxy, and the rest of the mass  $M$  is accumulated primarily during luminous accretion which has a low feedback energy coupling efficiency  $f_1$ , the average coupling efficiency is

$$f_{\text{av}} \sim \frac{\Delta M_{\text{obs}} + f_1 (M - \Delta M_{\text{obs}})}{M} = f_1 + (1 - f_1) \frac{\Delta M_{\text{obs}}}{M}. \quad (16)$$

If, for example, 10% of the SMBH mass is accumulated during heavily obscured phases, and the rest produces energy-driven outflows with  $f_1 = 0.05$ , we get  $f_{\text{av}} = 0.145$ , an almost threefold increase. Even if  $f_1 \sim 0$ , this results in  $f_{\text{av}} = 0.1$ , a value consistent with the derived prediction.

The fraction of mass that can be accreted during periods of strong obscuration is limited by the feedback energy. If most of the radiated energy is transferred to the ISM, it can be easily disrupted and expelled far away. The AGN is then no longer obscured and  $f_{\text{AGN}}$  decreases significantly. King & Muldrew (2016) estimate that the limiting mass for an AGN accreting in this hyper-Eddington mode is decreased from the usual  $M - \sigma$  value by a factor  $\sim \epsilon_{\text{AGN}}^{1/2} \dot{m}^{-1/2}$ , where  $\dot{m}$  is accretion rate in units of Eddington rate. The accretion rate must be  $\dot{m} \gg 1$  in order to produce strong obscuration, but cannot be too large so that the limiting mass does not become too small. Therefore, I predict that SMBHs grow  $\sim 10\%$  of their mass in heavily obscured phases with  $\dot{m} \gtrsim 10$ .

This prediction can be tested as more observations of obscured quasars are made. Obscured growth should occur at high redshift, because galaxies were more gas-rich then, making it easier to feed the SMBH at hyper-Eddington rates. Also, at high redshift the required  $f_{\text{AGN}}$  and  $f_{\text{p,AGN}}$  are lower, therefore it is easier to establish the SMBH-galaxy correlations. Both observations (Shields et al. 2006) and numerical simulations (Croton 2006) also suggest that black holes tend to grow faster than their host galaxies, consistent with the result that a lower  $f_{\text{AGN}}$  and  $f_{\text{p,AGN}}$  can establish

the observed galaxy mass function. Another prediction from this result is that the break in the galaxy mass function and the SMBH transition mass were established at  $z \gtrsim 2$ , consistent with observations (Behroozi et al. 2013).

An alternative explanation for high  $f_{\text{AGN}}$  would be that most AGN accretion occurs at very high radiative efficiency. This has two helpful consequences: the required  $f_{\text{AGN}}$  decreases because it is proportional to  $\epsilon_{\text{AGN}}^{-1}$ , and the actual  $f_{\text{AGN}}$  increases, because at least in the wind-driven outflow model, the fraction of energy transferred to the outflow is  $\sim \epsilon_{\text{AGN}}/2$ . If all SMBHs have maximal spins,  $\epsilon_{\text{AGN}} \sim 0.42$ , the energy transferred to the outflow increases by a factor 4.2, while the required  $f_{\text{AGN}}$  decreases by the same factor. This brings the two estimates into agreement.

There is some observational evidence that suggests typical values of  $\epsilon_{\text{AGN}}$  to be higher than the 10% assumed in the calculations above (Tombesi et al. 2010a,b, 2015; Veilleux et al. 2017). However, some theoretical arguments suggest that the opposite should be true (King et al. 2005; King & Pringle 2006). In addition, at least some of the accretion on to SMBHs happens in radiatively inefficient modes, so the total luminous output is less than the maximum possible. In addition, observed large-scale outflows have  $f_{\text{AGN}} \ll 0.05$  (Fiore et al. 2017), i.e. even if they are powered by rapidly spinning SMBHs, the energy communication is much weaker than the simple analytical estimate suggests. Therefore I think it is not very likely that the discrepancy can be explained purely by invoking high-spin SMBHs.

Finally, low-mass black holes can drive weak, but almost continuous, outflows in gas-poor galaxies, provided that the outflowing gas remains hot and approximately spherically symmetric (King & Pounds 2015). Although this process should only be important at low redshift and in small galaxies, which are presumably below the transition mass, it can nevertheless increase the total feedback energy injected into the ISM over the lifetime of a galaxy.

Some of the arguments presented above can be used, qualitatively at least, to explain the high values of  $f_{\text{p,AGN}}$  as well. Momentum injection is also increased by obscuration, by an even larger factor than energy injection, since high optical depth results in multiple photon scatterings and a global increase in scalar momentum. Furthermore, during highly obscured accretion, a large fraction of injected energy is predominantly kinetic, coming from hyper-Eddington winds, therefore the outflow momentum is also very large. On the other hand, increased radiative efficiency does not increase momentum injection, which is directly proportional to luminosity.

### 3.2 Selection effects

Another important reason for the discrepancy might be a range of selection effects that lead to observed  $f_{\text{AGN}}$  values being much lower than real ones, whether momentary or long-term average.

The most important selection effect may simply be redshift dependence of AGN outflows. As suggested above (Section 3.1), the connection between SMBH and the host galaxy may be established at high redshift, before or simultaneously with the peak of star formation rate density (Madau & Dickinson 2014). In this case, the outflows ob-

served in local galaxies are only much weaker analogues of outflows that actually quenched star formation in their host galaxies. This conclusion is supported by some observations which suggest that quasar-mode feedback is inefficient in low-redshift AGN (Shangguan et al. 2018). Current observations of massive outflows (Fiore et al. 2017) do not show any redshift dependence of coupling efficiency. However, molecular outflows, which seem to dominate the mass and energy budget, have been detected only at low redshift ( $z_{\text{mol}} < 0.2$ ) so far. If molecular outflows are detected in high-redshift galaxies, they should have higher energy coupling efficiencies and momentum loading factors compared with those in the local Universe.

It is also possible that each individual outflow goes through (potentially multiple) stages of high and low coupling efficiency, but outflows with low coupling efficiency are easier to observe. Low coupling efficiency might be observed for several reasons:

- If the AGN has recently (less than  $t_f \sim r/v$  ago, where  $r$  is the outflow radius and  $v$  is its radial velocity) increased its luminosity, the outflow has not had time to react to this change and will be seen as inefficiently coupled. Such a situation may have occurred if an AGN that had faded recently was later reinvigorated by another feeding event. In outflow samples selected by AGN luminosity, this effect may be important. A recently-increased AGN luminosity also means the Eddington ratio is higher, therefore a negative correlation between outflow coupling and Eddington ratio is expected in this case. This phenomenon is unlikely to explain most of the discrepancy, because a significant fraction of observed AGN are accreting at low Eddington ratios (Fiore et al. 2017, and references therein). However, some individual sources may show such behaviour, potentially identifiable by having several spatially distinct outflows (Nardini & Zubovas 2018).
- The outflow may have a higher coupling efficiency while its spatial extent is small ( $r \lesssim 100$  pc), due to higher average gas density and lower incidence of possible low-density gaps through which most of the feedback energy might escape (Nayakshin & Zubovas 2012; Zubovas & Nayakshin 2014). Outflows with low spatial extent are likely to be more obscured and therefore more difficult to detect, especially in gas-rich galaxies (Section 3.1; see also King & Muldrew 2016). On the other hand, numerical simulations suggest the opposite, that the total kinetic energy rate of outflows increases with increasing radius, therefore this explanation is unlikely to be universal either.
- A significant fraction of the outflow kinetic energy might be contained in material that is difficult to detect, for example due to low density, high ionisation, or rapid mixing with the galactic material making the outflowing material kinematically indistinguishable from undisturbed gas. This would mean that the observationally-derived coupling efficiencies are lower than real ones. However, non-molecular outflow components are observed to have much lower mass outflow rates, therefore their importance to the overall energy budget of the outflowing material is probably small (Tadhunter 2008; Morganti 2017).

To summarize, it seems that selection effects related to individual galaxies with outflows are unlikely to be able

to explain the discrepancy between observed and required values of  $f_{\text{AGN}}$ .

### 3.3 Uncertainties related to BHAR/SFR

The derived value of  $f_{\text{AGN}}$  and  $f_{\text{p,AGN}}$  is inversely proportional to the BHAR/SFR ratio, therefore uncertainties in that value can have a significant effect on the results. The ratio derived in Yang et al. (2017, 2018) is an underestimate to some extent, because broad-line and Compton-thick AGN were not included in that work. Type 1 AGN comprise  $\sim 20 - 30\%$  of all AGN (Lu et al. 2010), and the Compton-thick fraction is  $\sim 10 - 20\%$  (Akylas et al. 2012), therefore a total of  $\sim 30 - 50\%$  of AGN may be unaccounted for and the average BHAR may be underestimated by as much as a factor two. Correcting for this would lead to a reduction of both  $f_{\text{AGN}}$  and  $f_{\text{p,AGN}}$  by the same factor, bringing them closer to analytical predictions and observational constraints.

The correlation between BHAR and SFR has been the subject of much debate. While numerous authors found an almost linear (Chen et al. 2013) or somewhat sublinear (Diamond-Stanic & Rieke 2012) relation, spatially resolved analysis shows that the correlation is mainly observed on sub-kpc scales (LaMassa et al. 2013). Large sample analyses (Zheng et al. 2009) suggest that the correlation is only present in statistically averaged samples. Numerical simulations produce contrasting results, both in favour of the existence of correlations in individual galaxies (Hopkins & Quataert 2010) and against it, showing that the timescales of SFR and BHAR changes are too different for meaningful correlations to exist in individual galaxies (Hickox et al. 2014; Thacker et al. 2014; Volonteri et al. 2015). Overall, in individual galaxies on short timescales, the dominant feedback mechanism may be independent of galaxy mass. However, the argument presented in this paper depends only on the long-term energy injection by AGN and stellar feedback, therefore using long-term averages of BHAR and SFR is appropriate. Individual galaxies should generally show some correlation between long-term average BHAR and SFR values (Hopkins & Quataert 2010; Thacker et al. 2014), therefore the argument should hold on the scale of individual galaxies, and the uncertainty in the transition mass is predominantly caused by other factors than different timescale of BHAR and SFR variability.

The value of the transition mass between stellar- and AGN-dominated galaxies determines the appropriate BHAR/SFR ratio. It is also quite uncertain: Martin-Navarro & Mezcua (2018) give the mass as  $M_{\text{tr}} = 3.4 \pm 2.1 \times 10^{10} M_{\odot}$ . Taking the values of  $\dot{M}_{\text{BH}}/\dot{M}_{*}$  corresponding to the lower bound of  $M_{\text{tr}}$  gives  $0.093 < f_{\text{AGN}} < 1.14$ , while those corresponding to the upper bound give  $0.025 < f_{\text{AGN}} < 0.44$ . In either case, the difference is less than a factor 2 and is similar when individual  $\dot{M}_{\text{BH}}/\dot{M}_{*}$  trends at each redshift are considered. While the most optimistic scenario, i.e. a  $z > 2$  galaxy at the upper end of the allowed range for  $M_{\text{tr}}$ , gives  $f_{\text{AGN}}$  consistent with predictions of theoretical models, the tension with observed outflow properties remains unsolved. The variation of  $\dot{M}_{\text{BH}}/\dot{M}_{*}$  around the mean value at a given redshift is  $\pm 0.15$  dex for a galaxy sample at  $0.5 \leq z < 1.3$  (Yang et al. 2017). This factor  $\sim 1.4$  difference is lower than that associated with uncertainty in transition mass.

### 3.4 Uncertainties of stellar and AGN feedback efficiencies

There are also significant uncertainties inherent in the evaluation of the efficiency of stellar feedback (Krumholz et al. 2014). Feedback processes not included in the consideration above, such as photoionization feedback (e.g., Krumholz et al. 2006; Goldbaum et al. 2011), can control star formation in the host galaxy and thus have a strong effect on the total efficiency of stellar feedback, effectively adding another factor  $f_{\text{ph}} > 0$  to the term  $f_{\text{SN}} + f_{\text{w}}$ . Similarly, radiation pressure can add momentum to the gas, adding a factor  $f_{\text{rp}} > 0$  to  $f_{\text{p,SN}}$  and  $f_{\text{p,w}}$ . This would increase the estimated  $f_{\text{AGN}}$  and  $f_{\text{p,AGN}}$ , leading to even stronger tension with observations. On the other hand, geometrical effects of multiple-source feedback (Bourne & Power 2016) can reduce stellar feedback efficiency compared with single-source efficiency.

The fraction of massive star wind and supernova energy that is injected as kinetic energy into the ISM is also quite uncertain. Although the values used in the derivation here are based on detailed numerical simulations, some authors have argued for much lower actual coupling efficiencies,  $f_{\text{SN}} + f_{\text{w}} < 0.1$  (Fierlinger et al. 2016). These values are obtained from simulations of long-term evolution of ISM disturbed by winds and explosions of individual stars, although it is not straightforward to extrapolate these results to stellar populations with multiple feedback sources acting on long timescales. If  $f_{\text{SN}} + f_{\text{w}} = 0.1$  is used in eq. (10), the required AGN coupling efficiency becomes  $0.018 < f_{\text{AGN}} < 0.06$ , a range consistent with analytical models of AGN wind feedback and cosmological simulations, although still somewhat larger than values derived from real observed outflows.

AGN feedback may also manifest in other forms than, or in addition to, massive outflows, leading to higher actual values of  $f_{\text{AGN}}$  than outflow properties alone would suggest. Direct gas heating by the radiation field can be important, although probably only in gas-poor galaxies (Sazonov et al. 2005). Radiation pressure on the ISM can have significant effects (Ishibashi & Fabian 2014; Ishibashi et al. 2018), but these lead to outflows that should be observable similarly to wind-driven ones. Jet feedback can be very efficient compared to radiative output (Heinz et al. 2007; Mezcua & Prieto 2014), but it dominates only in low-luminosity sources (Heckman & Best 2014). In high-luminosity sources, such as radio-loud QSOs, jet feedback can at most produce as much power as radiative feedback, but typically has a radiative efficiency  $3 - 5 \times 10^{-3}$  (Merloni & Heinz 2008), i.e. is unlikely to increase  $f_{\text{AGN}}$  significantly. Furthermore, jet feedback mostly affects galaxies that have already ceased star formation, preventing circumgalactic material from falling back in. Overall, it appears that the energy input by AGN into the ISM of a gas-rich host galaxy is dominated by massive molecular outflows.

Some of the factors determining  $f_{\text{AGN}}$  and  $f_{\text{SN}} + f_{\text{w}}$  are the same, at least qualitatively, for both feedback processes. For example, in a clumpy galaxy, more energy may ‘leak out’ to large distances and have little effect on the process of star formation or SMBH feeding, independently of the origin of this energy (Zubovas & Nayakshin 2014; Recchi & Hensler 2006; Martizzi et al. 2015). The mass of the galactic halo

determines the conditions for outflow escape, and can lead to collapse of outflow bubbles, also independently of their origin. Therefore, conditions such as gas fraction or galaxy mass should not have a direct effect on the ratio between AGN and stellar feedback efficiencies; note that galaxy mass has a dominant effect on the BHAR-SFR ratio, which is what determines the transition mass between stellar- and AGN-dominated systems.

While the uncertainty of  $f_{\text{AGN}}$  and other coupling efficiencies involved is currently large, over time it should decrease as more detailed observations and numerical simulations are performed. Eventually, this may enable the use of such coupling efficiencies to investigate the variations in feedback efficiency among individual galaxies or their populations selected by certain parameters, such as stellar mass, morphology or environment. Assuming that the individual coupling efficiencies are independent of galaxy mass, one would be able to determine the relative importance of stellar and AGN feedback processes in any given galaxy and see how they correlate with other galaxy parameters. Alternatively, if the ratio of stellar-to-AGN power input  $R$  (eq. 3) can be determined for individual galaxies based on their mass compared to the transition mass, coupling efficiencies can be derived for individual galaxies, revealing the difference in how stellar and/or AGN feedback operates in galaxies with different properties.

### 3.5 Implications for individual galaxies across the mass range

The primary result of this paper, namely the large required value of  $f_{\text{AGN}}$  and  $f_{\text{p,AGN}}$ , is derived considering galaxies with  $R = 1$ , i.e. those at the transition between stellar- and AGN-dominated systems. Given the assumptions made in the derivation, namely that all coupling efficiencies are independent of galaxy mass, galaxies smaller (larger) than  $M_{\text{tr}}$  have  $R < 1$  ( $R > 1$ ) simply due to the increase of the BHAR-to-SFR ratio with mass (Yang et al. 2018). However, this assumption is not necessarily correct and individual galaxies may have AGN and/or stellar feedback coupled more or less strongly to the ISM than the average efficiencies described above. The reasons for these differences, and their consequences, might be the following:

- A small galaxy may be AGN dominated if its  $f_{\text{AGN}}$  is particularly large, or stellar feedback is particularly inefficient. This may be the case in a post-starburst galaxy, where numerous supernovae have recently opened chimneys and other channels for energy to leak out from most of the galactic volume (Recchi & Hensler 2006), but the central part is still gas-rich and feeds the AGN. Alternatively, a galaxy with low gas fraction, with low BHAR and SFR, may be more AGN-dominated if AGN feedback occurs via jets, which are more efficient than outflows in converting luminosity to mechanical energy (Heinz et al. 2007; Mezcuca & Prieto 2014). However, as mentioned above, such galaxies should already have their stellar and BH masses established.
- A large galaxy may be dominated by stellar feedback if its  $f_{\text{AGN}}$  is particularly small, or stellar feedback is particularly efficient. This may be the case if the AGN is fed slowly enough that a radiatively inefficient accretion flow develops (Yuan & Narayan 2014).

- A major gas-rich galaxy merger leads to a starburst, followed by a period of AGN activity after several times  $10^8$  yr. AGN feedback may then quench star formation or even enhance it (King & Pounds 2015). In addition, the changes in gas morphology due to the merger and its associated feedback can lead to wild variations in feedback coupling efficiencies. However, this effect should not be dominant to the establishment of galaxy-scale correlations, because mergers only contribute a small fraction to the total star formation and luminosity of galaxy population at any redshift (Hopkins et al. 2010).

All of these effects would lead to the transition between the two feedback regimes becoming more blurred. The large scatter of black hole masses around the transition region suggests that this is probably the case. Detecting individual galaxies where AGN or stellar feedback efficiencies are very different from the mean values would be possible with large data sets.

## 4 SUMMARY AND CONCLUSIONS

In this paper, I presented an empirical estimate of the AGN feedback coupling efficiency  $f_{\text{AGN}}$ , i.e. the fraction of AGN luminous energy output that is injected into the host galaxy ISM. This estimate relies only on two assumptions: that the total energy injected by AGN and by stellar feedback is the same for galaxies with stellar mass equal to the ‘break’, or transition, mass between stellar-feedback-dominated and AGN-dominated galaxies; and that the coupling efficiencies for AGN and stellar feedback processes are independent of galaxy mass. The estimated efficiency is, on average, very large,  $f_{\text{AGN}} > 0.045$ , and remains  $> 0.01$  even accounting for possible systematic uncertainties. Such high efficiency can only be achieved in very highly obscured AGN during the warm absorber phase, and perhaps in energy- or radiation-pressure-driven large-scale outflows. However, observed outflows typically have lower coupling efficiencies. A similar tension is seen when momentum loading is considered instead of energy injection: the required value  $f_{\text{p,AGN}} > 100$ , much higher than analytical or observational estimates.

There are several possible ways of resolving this tension:

- A significant fraction of total AGN feedback energy may be injected into the ISM during heavily obscured phases, when most of the luminous energy is used for driving the gas;
  - Selection effects may result in only inefficient outflows being observed, although this appears unlikely;
  - AGN-induced quenching of star formation may have happened predominantly at high redshift ( $z > 2$ ), and outflows observed in the local Universe are quantitatively very different from those that actually quenched their galaxies;
  - Stellar feedback coupling efficiencies might be significantly lower than those used in calculating this estimate.

None of these possibilities is mutually exclusive with any other.

As observational data become better and detailed numerical simulations provide ever more information on the relevant coupling efficiencies, an estimate of  $f_{\text{AGN}}$  such as provided in this paper may be used to test various feedback

models and to analyse variations in feedback among different galaxy sub-populations.

## ACKNOWLEDGMENTS

I thank Sergei Nayakshin, Andrew King, Mar Mezcua and Guang Yang for helpful suggestions during the preparation of this manuscript. I also thank the anonymous referee for insightful comments that helped improve the clarity of the arguments presented here. This research was funded by a grant (No. LAT-09/2016) from the Research Council of Lithuania.

## REFERENCES

- Agertz O., Kravtsov A. V., Leitner S. N., Gnedin N. Y., 2013, *ApJ*, 770, 25
- Akylas A., Georgakakis A., Georgantopoulos I., Brightman M., Nandra K., 2012, *A&A*, 546, A98
- Behroozi P. S., Wechsler R. H., Conroy C., 2013, *ApJ*, 770, 57
- Booth C. M., Schaye J., 2009, *MNRAS*, 398, 53
- Bourne M. A., Power C., 2016, *MNRAS*, 456, L20
- Chabrier G., 2003, *ApJL*, 586, L133
- Chen C.-T. J., Hickox R. C., Alberts S., Brodwin M., Jones C., Murray S. S., Alexander D. M., Assef R. J., Brown M. J. I., Dey A., Forman W. R., Gorjian V., Goulding A. D., Le Floch E., Jannuzi B. T., Mullaney J. R., Pope A., 2013, *ApJ*, 773, 3
- Croton D. J., 2006, *MNRAS*, 369, 1808
- Diamond-Stanic A. M., Rieke G. H., 2012, *ApJ*, 746, 168
- Fierlinger K. M., Burkert A., Ntormousi E., Fierlinger P., Schartmann M., Ballone A., Krause M. G. H., Diehl R., 2016, *MNRAS*, 456, 710
- Fiore F., Feruglio C., Shankar F., Bischetti M., Bongiorno A., Brusa M., Carniani S., Ciccone C., Duras F., Lamastra A., Mainieri V., Marconi A., Menci N., Maiolino R., Piconcelli E., Vietri G., Zappacosta L., 2017, *A&A*, 601, A143
- Goldbaum N. J., Krumholz M. R., Matzner C. D., McKee C. F., 2011, *ApJ*, 738, 101
- Harrison C. M., 2017, *Nature Astronomy*, 1, 0165
- Heckman T. M., Best P. N., 2014, *ARA&A*, 52, 589
- Heinz S., Merloni A., Schwab J., 2007, *ApJL*, 658, L9
- Hickox R. C., Mullaney J. R., Alexander D. M., Chen C.-T. J., Civano F. M., Goulding A. D., Hainline K. N., 2014, *ApJ*, 782, 9
- Hopkins P. F., Quataert E., 2010, *MNRAS*, 407, 1529
- Hopkins P. F., Younger J. D., Hayward C. C., Narayanan D., Hernquist L., 2010, *MNRAS*, 402, 1693
- Ishibashi W., Fabian A. C., 2014, *MNRAS*, 441, 1474
- Ishibashi W., Fabian A. C., Maiolino R., 2018, *MNRAS*, 476, 512
- King A., 2003, *ApJL*, 596, L27
- King A., Muldrew S. I., 2016, *MNRAS*, 455, 1211
- King A., Pounds K., 2015, *ARA&A*, 53, 115
- King A. R., 2010, *MNRAS*, 402, 1516
- King A. R., Lubow S. H., Ogilvie G. I., Pringle J. E., 2005, *MNRAS*, 363, 49
- King A. R., Pounds K. A., 2014, *MNRAS*, 437, L81
- King A. R., Pringle J. E., 2006, *MNRAS*, 373, L90
- Kormendy J., Fisher D. B., Cornell M. E., Bender R., 2009, *ApJS*, 182, 216
- Kormendy J., Ho L. C., 2013, *ARA&A*, 51, 511
- Krumholz M. R., Bate M. R., Arce H. G., Dale J. E., Guter-muth R., Klein R. I., Li Z.-Y., Nakamura F., Zhang Q., 2014, *Protostars and Planets VI*, pp 243–266
- Krumholz M. R., Matzner C. D., McKee C. F., 2006, *ApJ*, 653, 361
- LaMassa S. M., Heckman T. M., Ptak A., Urry C. M., 2013, *ApJL*, 765, L33
- Leitherer C., Robert C., Drissen L., 1992, *ApJ*, 401, 596
- Lu Y., Wang T.-G., Dong X.-B., Zhou H.-Y., 2010, *MNRAS*, 404, 1761
- Madau P., Dickinson M., 2014, *ARA&A*, 52, 415
- Martin-Navarro I., Mezcua M., 2018, *ArXiv e-prints*
- Martizzi D., Faucher-Giguère C.-A., Quataert E., 2015, *MNRAS*, 450, 504
- McGaugh S. S., 2005, *ApJ*, 632, 859
- Merloni A., Heinz S., 2008, *MNRAS*, 388, 1011
- Mezcua M., Prieto M. A., 2014, *ApJ*, 787, 62
- Morganti R., 2017, *ArXiv e-prints*
- Moster B. P., Naab T., White S. D. M., 2013, *MNRAS*, 428, 3121
- Murray N., Quataert E., Thompson T. A., 2005, *ApJ*, 618, 569
- Nardini E., Zubovas K., 2018, *MNRAS*
- Nayakshin S., Zubovas K., 2012, *MNRAS*, 427, 372
- Puchwein E., Springel V., 2013, *MNRAS*, 428, 2966
- Recchi S., Hensler G., 2006, *A&A*, 445, L39
- Rosdahl J., Schaye J., Teyssier R., Agertz O., 2015, *MNRAS*, 451, 34
- Rosen A. L., Lopez L. A., Krumholz M. R., Ramirez-Ruiz E., 2014, *MNRAS*, 442, 2701
- Sazonov S. Y., Ostriker J. P., Ciotti L., Sunyaev R. A., 2005, *MNRAS*, 358, 168
- Schaye J., Crain R. A., Bower R. G., Furlong M., Schaller M., Theuns T., Dalla Vecchia C., Frenk C. S., McCarthy I. G., et al. 2015, *MNRAS*, 446, 521
- Schaye J., Dalla Vecchia C., Booth C. M., Wiersma R. P. C., Theuns T., Haas M. R., Bertone S., Duffy A. R., McCarthy I. G., van de Voort F., 2010, *MNRAS*, 402, 1536
- Shangguan J., Ho L. C., Xie Y., 2018, *ApJ*, 854, 158
- Shankar F., Lapi A., Salucci P., De Zotti G., Danese L., 2006, *ApJ*, 643, 14
- Shields G. A., Salviander S., Bonning E. W., 2006, *NewAR*, 50, 809
- Somerville R. S., Davé R., 2015, *ARA&A*, 53, 51
- Tadhunter C., 2008, *Mem. della SAI*, 79, 1205
- Thacker R. J., MacMackin C., Wurster J., Hobbs A., 2014, *MNRAS*, 443, 1125
- Thornton K., Gaudlitz M., Janka H.-T., Steinmetz M., 1998, *ApJ*, 500, 95
- Tombesi F., Cappi M., Reeves J. N., Palumbo G. G. C., Yaqoob T., Braitto V., Dadina M., 2010a, *A&A*, 521, A57+
- Tombesi F., Meléndez M., Veilleux S., Reeves J. N., González-Alfonso E., Reynolds C. S., 2015, *Nature*, 519, 436
- Tombesi F., Sambruna R. M., Reeves J. N., Braitto V., Ballo L., Gofford J., Cappi M., Mushotzky R. F., 2010b, *ApJ*, 719, 700
- Tully R. B., Fisher J. R., 1977, *A&A*, 54, 661



- Veilleux S., Bolatto A., Tombesi F., Meléndez M., Sturm E., González-Alfonso E., Fischer J., Rupke D. S. N., 2017, *ApJ*, 843, 18
- Vogelsberger M., Genel S., Springel V., Torrey P., Sijacki D., Xu D., Snyder G., Nelson D., Hernquist L., 2014, *MNRAS*, 444, 1518
- Volonteri M., Capelo P. R., Netzer H., Bellovary J., Dotti M., Governato F., 2015, *MNRAS*, 449, 1470
- Walch S., Naab T., 2015, *MNRAS*, 451, 2757
- Yang G., Brandt W. N., Vito F., Chen C.-T. J., Trump J. R., Luo B., Sun M. Y., Xue Y. Q., Koekemoer A. M., Schneider D. P., Vignali C., Wang J.-X., 2018, *MNRAS*, 475, 1887
- Yang G., Chen C.-T. J., Vito F., Brandt W. N., Alexander D. M., Luo B., Sun M. Y., Xue Y. Q., Bauer F. E., Koekemoer A. M., Lehmer B. D., Liu T., Schneider D. P., Shemmer O., Trump J. R., Vignali C., Wang J.-X., 2017, *ApJ*, 842, 72
- Yuan F., Narayan R., 2014, *ARA&A*, 52, 529
- Zheng X. Z., Bell E. F., Somerville R. S., Rix H.-W., Jahnke K., Fontanot F., Rieke G. H., Schiminovich D., Meisenheimer K., 2009, *ApJ*, 707, 1566
- Zubovas K., King A., 2012, *ApJL*, 745, L34
- Zubovas K., Nayakshin S., 2014, *MNRAS*, 440, 2625